Journal of Computer-Aided Molecular Design, **12:** 195–213, 1998.
KLUWER/ESCOM

Conformational analysis of [Met^5]-enkephalin: Solvation and ionization considerations

Louis Carlacci
Department of Chemistry, CHE 305, University of South Florida, Tampa, FL 33620–5250, U.S.A.

Received 24 June 1997; Accepted 5 November 1997

Key words: conformational search, conformer inter-conversion, entropy, neuropeptide, pharmacophore mapping, thermodynamics

Summary

[Met^5]-Enkephalin has the sequence Tyr-Gly-Gly-Phe-Met. Only the extended conformation of the peptide has been observed by X-ray crystallography. Nuclear magnetic resonance spectroscopy supports the presence of a turn at Gly 3 and Phe 4 in dimethyl sulfoxide. In this study, the peptide conformational states and thermodynamic properties are understood in terms of ionization state and solvent environment. In the calculation, final conformations obtained from multiple independent Monte Carlo simulated annealing conformational searches are starting points for molecular dynamics simulations. In an aqueous environment given by the use of solvation free energy and the zwitterionic state, dominant structural motifs computed are G-P Type II′ bend, G-G Type II′ bend, and G-G Type I′ bend motifs, in order of increasing free energy. In the calculation of the peptide with neutral N- and C-termini and solvation free energy, the extended conformer dominates (by at least a factor of 2.5), and the conformation of another low free energy conformer superimposes well on the pharmacophoric groups of morphine. Neutralization of charge and solvation induce and stabilize the extended conformation, respectively. A mechanism of inter-conversion between the extended conformer and three bent conformers is supported by ϕ/ψ-scatter plots, and by the conformer relative free energies. An estimate of the entropy change of receptor unbinding is 8.3 cal K^{-1} mol^{-1}, which gives rise to a -2.5 kcal/mol entropy contribution to the free energy of unbinding at 25 °C. The conformational analysis methodology described here should be useful in studies on short peptides and flexible protein surface loops that have important biological implications.

Introduction

[Met^5]-Enkephalin (Met-Enk) is a five-residue endogenous opiate peptide for which the amino acid sequence is Tyr-Gly-Gly-Phe-Met [1]. Enkephalins bind preferentially to δ-receptors and show some affinity for μ- (or morphine) receptors. The precise bioactive conformation of the peptide has eluded identification. The possibility exists that enkephalins bind to δ- and μ-receptors by assuming two distinct conformations. The membrane environment of the receptor could induce the specific conformation of the peptide that binds the receptor [2]. Based on conformation-activity relationships determined for enkephalins, the important pharmacophoric requirements of μ-receptor binding are the positions and orientations of the aromatic side chains, and the relationship of the N-terminus nitrogen to the oxygen of the phenol [3, 4].

Crystal data on opiate peptides and their biological activity were recently reviewed by Deschamps et al. [5]. In the solid state, only one conformation of the peptide has been determined by X-ray crystallography, the extended conformation. Nuclear magnetic resonance spectroscopy (NMR) on the peptide in dimethyl sulfoxide supports the presence of a turn at Gly 3 and Phe 4 with a hydrogen bond (H-bond) between Gly 2 and Met 5 [6–9]. An NMR structure determined at pH≅4 showed a β-turn in a 'lipid-like' SDS solution, and no stable secondary structure in aqueous solution [10].

Goals of past theoretical calculations were to determine the global minimum energy conformation of

the peptide, and to improve the efficiency of computation for this conformation [11–19]. The global minimum energy conformation computed in a vacuum with neutral N- and C-termini has a G-P Type II′ β-turn [11], where 'G-P' stands for Gly 3 and Phe 4. (The present study employs the β-turn nomenclature in the review by Richardson [20].) In molecular dynamics (MD) simulations that employed a distance dependent dielectric (called R-dielectric) starting from the extended conformation of the peptide in the zwitterionic state, the most stable conformer observed by Ishida et al. [18] was a G-G Type II′ β-turn. Perez et al. [19] computed conformational searches on the neutral peptide in an apolar environment, represented by an R-dielectric. Perez found the global minimum energy conformation and β-turn conformations higher in energy. The present study provides a conformational and thermodynamic analysis that considers neutral and zwitterionic peptide ionization states, and solvation free energy versus just an R-dielectric. The Monte Carlo simulated annealing (MCSA) conformational search approach developed and implemented by Carlacci and Englander [22, 23] for the calculation of protein surface loops starting from random conformations is employed in the present study. The MCSA approach accurately predicted the native X-ray conformations of five-residue loops on the protein surface. An MCSA run starts out with a high Boltzmann temperature factor, RT (in kcal/mol). In the course of a run, many trial conformations are sequentially evaluated. As the temperature factor is gradually lowered at intervals during a run, the conformational search is restricted to lower energy conformational search pathways.

The calculation in the present study has two parts, conformational search and molecular dynamics. Conformational searches for the lowest energy conformations are computed by multiple independent MCSA runs starting from random conformations. Conformations saved during MD runs starting from MCSA final conformations are employed in equilibrium thermodynamic analyses.

The thermodynamic analyses used in studies of protein unfolding and receptor binding are analogous in some ways. Based on the thermodynamic analysis by Makhatadze and Privalov [21], the entropy of protein unfolding is the sum of the configuration entropy, and the entropy of hydration of polar and nonpolar groups. The configuration entropy of protein unfolding is a positive quantity. The protein unfolding entropies due to hydration of polar and non-polar groups are both negative. Based on the analysis by Makhatadze and Privalov, the entropy computed in this study is not just the configuration entropy, which is determined in vacuum. The entropy due to hydration of polar and non-polar groups is not incorporated in the entropy computed here, where the computed entropy of a rigid conformation is zero, even when solvation free energy is used in the calculation. The computed entropy in this study is described as the sum of the configuration entropy and the entropy due to the correlation between peptide configuration and hydration of polar and non-polar groups. The unfolding entropies due to hydration of polar and non-polar groups referred to by Makhatadze and Privalov include the entropy due to the correlation between peptide configuration and hydration. An estimate of the entropy of receptor unbinding is the difference between the entropy of the free peptide in an aqueous environment and the entropy of a rigid bound conformation.

One of the goals in the present study is to better understand the effects of ionization and solvent environment. The solvent environments considered are apolar (or lipid), by the use of an R-dielectric, and polar (or aqueous), by the use of solvation free energy based on solvent accessible surface. Ionization states explored are the neutral N- and C-termini state (called the n/n-state) and the zwitterionic state (called the i/i-state). Four calculations are systematically obtained, namely, solvation and R-dielectric calculations of i/i-Met-Enk and n/n-Met-Enk. The solvation calculation of i/i-Met-Enk is the calculation used to describe the peptide in an aqueous solution. The R-dielectric calculation of n/n-Met-Enk is the calculation used to describe the peptide in a 'lipid-like' environment. Calculations of n/n-Met-Enk assume one or more neutralization mechanisms exist. In one possible mechanism, the low dielectric of the receptor (or crystal) shifts the pK of the C-terminus proton up, and the pK of the N-terminus proton down. Neutralization at the N- and C-termini could be accomplished by ionic interactions.

The present study contains results that to the best of the author's knowledge have not been previously exposed. Up until the present study, a low energy extended conformation of the peptide has not been reported; and other calculations do not support a mechanism of inter-conversion between Met-Enk conformers. In the solvation calculation of n/n-Met-Enk, the extended conformer is the most populated conformer by a factor of 2.5; and the conformation of another low energy conformer satisfies the important

pharmacophoric requirements for μ-receptor binding. The effect that ionization and solvation have on the peptide conformational states, and on the stability of the extended conformation of the peptide is better understood.

Another goal of the study is to develop and implement a strategy for the conformational analysis of short peptides and flexible protein surface loops. This study implements a new approach to the solution of some old problems. The questions answered in the present study are: (a) How can similar conformations be identified and grouped into a conformer? (b) What are the entropy and relative free energy of dominant conformers? and (c) How can conformational changes be characterized in terms of structure and thermodynamics? The knowledge and expertise obtained in the present study should be useful in studies of short peptides and flexible protein surface loops.

Methods

Coordinates and energy function

The peptide geometry is generated by the ECEPP/2 protocol, in which bond lengths and bond angles are held fixed, and dihedral angles may vary [24]. L-Amino acids are employed. Explicit water molecules are not considered.

The total energy, F, is given by

$$F = E + J, \tag{1}$$

where E is the peptide conformational energy [24] computed with CHARMm parm 20 all atom energy parameters [25] and J is the solvation free energy. The conformational energy is the sum of Lennard-Jones non-bonded, electrostatic and torsion potentials. The hydrogen bond energy is built into the nuclear charges. In all calculations, nuclear charges are screened by the use of an R-dielectric ($e = r$, where r is the interatomic distance). The R-dielectric has the dielectric properties of the protein interior (or crystal) for small r, and approaches the dielectric properties of water ($e = 80$) as r increases. In calculations that include solvation, the solvation free energy is given by

$$J = \sum_{i=1}^{N} A_i \sigma_i, \tag{2}$$

where A_i is the solvent accessible surface area of atom i and s_i is the atom solvation parameter. The SRFOPT parameter set [26] is employed along with parameters for charged atoms [27]. Solvent accessible surface area is computed with a module called MSEED [28].

The solvation parameters used are designed for water as solvent. The solvation parameters for nitrogen, and oxygen, as well as carbon of $–CH_2–$, and aromatic =CH–, which are present in Tyr 1, Phe 4 and Met 5 side chains, give rise to a negative solvation free energy. The solvation free energy contribution of Met 5 $–CH_3$ is positive.

Conformational search and molecular dynamics protocols

There are many implementations of MCSA in the literature (see Ref. 22 for a list). In the inner loop of an MCSA run (called an MCSA cycle) a trial conformation is generated, and the total energy is computed. The energy of the trial conformation is compared to the energy of the previously accepted conformation. The trial conformation is accepted if its total energy is less than or equal to the total energy of the currently accepted conformation. Otherwise, the Metropolis criterion is used to accept or reject the current trial conformation [29]. The most recently accepted trial conformation is used at the start of the next cycle.

An MCSA run starts out with a large Boltzmann temperature factor (RT in kcal/mol). In a simulated annealing step, RT_i, the temperature factor at step i in the annealing, is fixed; and a number of trial conformations (NCON) are evaluated. At the end of each step, the current temperature factor is lowered. The run is stopped after a specified number of steps, NSTEP.

A calculation loops through 500 independent MCSA runs. Each run consists of an equilibration stage starting from a random conformation followed by a prediction stage. The value of RT at the start of the equilibration stage produces a thorough conformational search as determined by a scatter plot of accepted ϕ/ψ conformations. Main chain and side chain trial conformations are evaluated using separate Boltzmann temperature factors. In the previous implementation [22], multiple prediction runs started from the final conformations of several equilibration runs; and one Boltzmann temperature factor was employed. The rest of the MCSA protocol employed here is the same as that employed in Ref. 22; see Table 1.

A trial conformation is generated by the random walk method in which a randomly selected dihedral angle is randomly assigned a new value inside a range defined by the current perturbation. Any dihedral an-

Table 1. Protocol used in each of the 500 independent MCSA runs

Parameter	Equilibration stage	Prediction stage
NSTEP	11 steps	14
NCON	1500 trial conformations	1500
RT	main chain: from 8.0 to 4.0 kcal/mol main chain: from 4.0 to 0.6 kcal/mol	side chain: from 4.0 to 0.6 kcal/mol side chain: from 2.0 to 0.6 kcal/mol
Perturbations	$\pm 180°$ backbone, $\pm 180°$ side chain	final perturbations of equilibration stage

gle, ϕ, ψ, ω or χ's, can be randomly selected. The current perturbation is reduced by a factor of 2.0 if the fraction of trial conformations accepted is below the acceptance ratio limit, which is 25% for main chain and 40% for side chain trial conformations. Values of NCON and NSTEP chosen are based on experience.

A conformational search calculation is converged when the final conformations of many independent MCSA runs converge on the same low energy conformers.

Algorithms that reduce the conformational search effort [22] are: (a) varying dihedral angles in pairs, (b) the use of main chain and side chain rotamers, and (c) altering the rate at which main chain and side chain dihedral angles are selected. In varying dihedral angles in pairs, if ϕ (or ψ) of residue i is selected then both ϕ_i and ψ_{i-1} (or ϕ_{i-1} and ψ_i) are assigned values; and both χ_1 and χ_2 are assigned values if either is selected. Side chain rotamers are defined for each side chain dihedral angle. In the use of the side chain rotamer option, side chain dihedral angles with one rotamer conformation are fixed, otherwise, a rotamer conformation is randomly selected. Statistical weights based on the frequency of occurrence of a side chain rotamer conformation in the X-ray data [30] are employed in the selection of χ_1 and χ_2. The side chain rotamer option is turned off when the side chain RT is less than 1.5 kcal/mol (at step 15). Rotamer conformations for ω, and the ϕ/ψ pair are employed. In the use of the ω rotamer option, only cis ($0°$) and trans ($180°$) conformations are allowed. Trans to cis transitions occur with a 10% probability; and cis to trans transitions are always allowed. The ω rotamer option is turned off when the main chain RT is less than 2.0 kcal/mol (at step 17). In the use of the ϕ/ψ rotamer option, ϕ/ψ rotamer values are chosen when either ϕ or ψ is selected. The ϕ/ψ rotamers are α-helix and β-strand rotamers, and β-turn rotamers compiled from X-ray data [31, 32]. The ϕ/ψ rotamer option is turned off when the main chain RT is less than 6.4 kcal/mol (at step 5). In the use of the selection rate option, the probability that a main chain conformation is evaluated is increased from 0.65 to 0.75; and the probability that a side chain conformation is evaluated is decreased from 0.35 to 0.25. The selection rate option is turned off when the main chain RT is less than 2.0 kcal/mol (at step 17).

Final conformations of MCSA runs are starting points for Monte Carlo MD runs. At the end of the equilibration step, the current perturbation is reduced by a factor of 1.5 if the fraction of trial conformations accepted is below the acceptance ratio limit, which is 40% for both main chain and side chain trial conformations. During the MD production step, conformations for analysis are saved in intervals of 250 trial conformations (see Table 2).

Thermodynamic characterization

The conformational analysis program (called Popen), which is written in the C language, groups similar conformations into conformers, generates ϕ/ψ scatter plots for each residue, and calculates the entropy and Boltzmann average properties of conformers. Program Popen first assigns each residue of a saved conformation alpha-numeric tags (called rotamer tags) that specify the conformations of the ϕ/ψ pair, ω, and each χ. The ϕ/ψ rotamer conformations are given in Figure 1. Rotamer conformations of ω are $180° \pm 55°$, $0° \pm 55°$, $90° \pm 35°$, and $-90° \pm 35°$. Tyr χ_1, Phe χ_1, and Met χ_1, χ_2 and χ_3 each have three rotamer conformations, namely, –60°, 180° and 60°. Tyr χ_3 has two rotamer conformations, namely, 0° and 180°. Met χ_4, Tyr χ_2, and Phe χ_2 each have one rotamer conformation, namely, $60° \pm 60°$, $90° \pm 90°$, and $90° \pm 90°$, respectively. The symmetry of the phenol ring allows Tyr χ_2 to lie in the range $90° \pm 90°$ by addition of 180° to χ_2, and subtraction of 180° from

Table 2. Protocol used in Monte Carlo MD runs (RT=0.6 kcal/mol)

Parameter	Equilibration step	Production step
NCON	15000 trial conformations	25000
Perturbations	±10° backbone, ±30° side chain	final perturbations of equilibration step

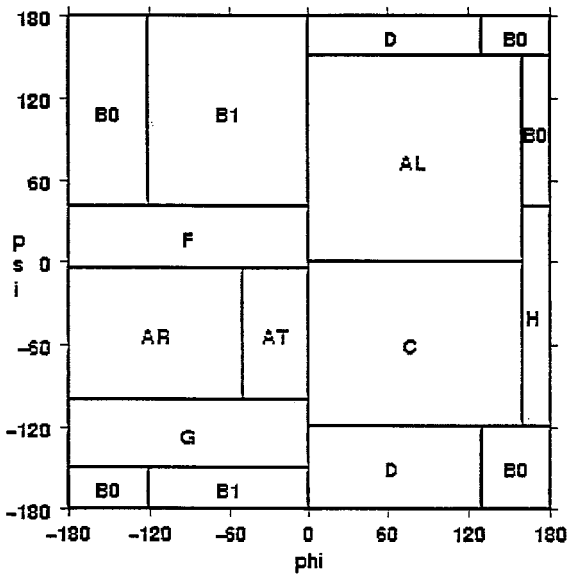

Figure 1. Ramachandran plot, defining the ϕ/ψ rotamer regions used to identify main chain conformations of individual residues.

χ_3. A group of conformations with the same sequence of main chain rotamer tags is called a main chain conformer; and a group of conformations with the same sequence of main chain and side chain rotamer tags is called a main chain/side chain conformer.

The nomenclature used to identify β-turn conformations is summarized in Table 3. Column one gives the β-turn type; and columns 2 to 5 give the ideal ϕ/ψ values of the two turn residues. Definitions of β-turn types in terms of the Ramachandran nomenclature and in terms of main chain rotamer tags are given in columns 6 and 7, respectively. For simplification, a B rotamer tag denotes either B0 or B1 β-strand regions; and an A rotamer tag denotes either AR or AT α-helix regions. In this study, a Type II′ bend conformer is identified as four sequential residues with the B_C_A_(A or B) or B_C_B_B sequence of main chain rotamer tags, regardless of the H-bond pattern between the first and last residues. The use of β-turn following the turn type implies H-bonds between residues appended to the turn residues [20].

The Boltzmann averaged properties computed are average total energy and average conformation in terms of dihedral angles. Boltzmann averaged conformations are computed for main chain / side chain conformers. The Boltzmann average property, $\overline{\mathrm{W}}$, is given by

$$\overline{W} = \frac{1}{Q}\sum_i W_i \exp^{-F_i/RT} , \tag{3}$$

where W_i is the property of conformation i, F_i is the total energy of conformation i, R is the gas constant, 1.987 cal K^{-1} mol^{-1}, T is 300 K, and the partition function, Q, is

$$Q = \sum_i \exp^{-F_i/RT} \tag{4}$$

Based on the canonical ensemble, the entropy, S, and free energy, A, are

$$S = R \ln Q + \frac{1}{TQ}\sum_i F_i \exp^{-F_i/RT} \tag{5}$$

and

$$A = -RT \ln Q . \tag{6}$$

A programming adaptation that circumvents errors in precision is to convert the total energies that appear in the exponents of Equations (3) to and (6) into relative total energies, or $F_\mathrm{i} - F_\mathrm{LEC}$, where F_LEC is the total energy of the lowest energy conformation. The total energies are expressed in terms of relative total energies by multiplying each equation by the identity,

$$\frac{\exp^{-F_\mathrm{LEC}/RT}}{\exp^{-F_\mathrm{LEC}/RT}} .$$

Table 3. Nomenclature for ideal 2-residue β-turn loops

β-turn type[a]	φ/ψ-dihedral angles [b]				Ramachandran nomenclature[c]	Main chain rotamer tag nomenclature[d]
	ϕ_i	ψ_i	ϕ_{i+1}	ψ_{i+1}		
Type I	–60	–30	–90	0	$\alpha_R \rightarrow \alpha_R$	B_A_A_(A or B)
Type I′	60	30	90	0	$\alpha_L \rightarrow \gamma_L$	B_AL_C_(A or B), B_C_C_(A or B)
Type II	–60	120	80	0	$\beta \rightarrow \alpha_L$	B_B_AL_(A or B), B_B_C_(A or B)
Type II′	60	–120	–80	0	$\epsilon \rightarrow \alpha_R$	B_C_A_(A or B), B_C_B_(A or B)

[a] β-turn type as defined in Ref. 20.
[b] Ideal values of φ/ψ-dihedral angles for the 2 residues of the β-turn.
[c] Ramachandran regions as given in Ref. 32.
[d] Main chain rotamer tags of four sequential residues that identify the bend motif given in column 1 (see also Figure 1). The rotamer tag nomenclature assumes trans conformation of peptide ω.

Results

Convergence of the conformational search calculations

Convergence of MCSA runs in solvation calculations is demonstrated in Table 4. Column 1 is the conformer number ordered in terms of increasing free energy. Column 2 is the conformer population in terms of number of final conformations. Columns 3 and 4 are the relative free energy and entropy, respectively. Columns 5 to 9 give the residue main chain rotamer tags, starting at the N-terminus. Due to space limitations, only the 15 lowest energy main chain conformers are characterized.

In solvation calculations, program Popen finds 192 and 277 main chain conformers of i/i-Met-Enk and n/n-Met-Enk, respectively. Based on the 15 lowest free energy main chain conformers of i/i-Met-Enk, 111 runs led to G-G Type I′ bend conformations (conformers 1, 3, 5, 6, 7, and 14); 89 runs led to G-G Type II′ bend conformations (conformers 2, 4, and 15); and 73 runs led to G-P Type II′ bend conformations (conformers 8, 9, 13, and 16). In the calculation of n/n-Met-Enk, 41 runs led to G-G Type II′ bend conformations (conformers 1, 13, and 14); 169 runs led to extended chain conformations (conformers 3, 6, 9, and 10); and 11 runs led to G-G Type II bend conformations (conformers 4, 8, and 12). Main chain conformers higher in energy are not nearly as populated. For solvation and R-dielectric calculations, conformations of conformers less than 7.5 and 15 kcal/mol in relative free energy, respectively, are starting points for MD runs.

Thermodynamic properties of Met-Enk

In solvation calculations of i/i-Met-Enk and n/n-Met-Enk, 370 and 384 MD runs, respectively, are computed; and 37000 and 38400 conformations, respectively, are saved for analysis. Conformational analyses of i/i-Met-Enk and n/n-Met-Enk yielded 647 and 1993 main chain conformers, respectively, and 7123 and 14295 main chain/side chain conformers, respectively. In R-dielectric calculations of i/i-Met-Enk and n/n-Met-Enk, 382 and 340 MD runs, respectively, are computed; and 38200 and 34000 conformations, respectively, are saved for analysis. Conformational analyses of i/i-Met-Enk and n/n-Met-Enk yielded 761 and 2343 main chain conformers, respectively, and 10878 and 14756 main chain/side chain conformers, respectively.

Thermodynamic properties of conformers with a common structural motif (called motif conformers) are reported in Tables 5 to 8. Columns 1 to 5 are the conformer number, conformer population in terms of number of conformations saved during the MD runs, relative total energy, relative free energy, and entropy, respectively. Columns 6 to 10 are main chain rotamer tags. An X rotamer tag implies any rotamer conformation in Figure 1. Thermodynamic properties of all conformations, the ensemble relative total energy, ensemble relative free energy, and ensemble entropy, are given in the last row.

In the solvation calculation of i/i-Met-Enk, the lowest free energy conformer has a G-P Type II′ bend (conformer 1 in Table 5). G-G Type II′ bend conformers (conformers 4 and 5) and G-G Type I′ bend conformers (conformers 6 and 7), which are significantly populated, are about 1.4 and 2.2 kcal/mol higher in free energy, respectively. Based on the computed entropy of the dominant conformers, the G-G Type I′ bend conformer has the largest density of conformational states.

In the solvation calculation of n/n-Met-Enk, a G-G Type II′ bend conformer (conformer 1 in Table 6)

Table 4. Convergence of 500 independent MCSA conformational searches that include solvation[a]

i/i-Met-Enk									n/n-Met-Enk								
M[b]	ncon[c]	Δ A[d]	S[e]	MC rotamer tags [f]					M[b]	ncon[c]	Δ A[d]	S[e]	MC rotamer tags [f]				
1	22	0.0	2.2	B	AL	C	B	B	1	18	0.0	2.1	B	C	B	B	B
2	40	0.7	2.6	A	B	C	A	B	2	1	0.4	0.0	B	B	A	B	A
3	60	1.3	3.4	B	AL	C	A	B	3	46	0.8	4.0	AL	B	B	B	B
4	26	1.5	3.0	B	B	C	A	B	4	1	0.9	0.0	B	B	C	A	B
5	7	1.7	2.0	B-	AL	C	A	B	5	4	0.9	0.4	D	C	B	B	A
6	1	1.7	0.0	B	AL–	AL	B+	B	6	39	0.9	0.5	B	B	B	B	A
7	15	2.1	2.4	B	AL	C	B	AL	7	1	1.1	0.0	AL	B	A	A	B
8	26	2.3	3.7	B	C	A	B	B	8	4	1.2	0.0	B	B	C	B	A
9	11	2.4	1.1	B	C	A	B	AL	9	41	1.6	4.3	AL	B	B	B	A
10	3	2.7	1.4	A	A	G	A	B	10	43	1.6	3.6	B	B	B	B	B
11	1	2.7	0.0	A	D	C	A	B	11	9	1.6	2.1	D	C	B	B	B
12	2	3.0	0.4	A	B	A	A	B	12	6	1.8	0.0	AL	B	C	B	B
13	48	3.1	3.6	B	C	A	A	B	13	20	2.0	1.8	B	C	B	B	A
14	6	3.1	0.1	B	AL	H	A	B	14	3	2.8	0.0	B	C	B	A	B
15	9	3.9	1.8	B+	B	C	A	B	15	1	3.0	0.0	B	AL	C	A	B+

[a] Fifteen lowest free energy conformers obtained from final conformations of 500 MCSA runs.
[b] Conformer number ordered by increasing energy.
[c] Conformer population in terms of number of final conformations.
[d] Relative free energy in kcal/mol. See Equation 6.
[e] Entropy (in cal K^{-1} mol^{-1}). See Equation 5.
[f] Main chain rotamer tag of each residue from N- to C-terminus (see also Figure 1). Appended superscripts specify conformations of ω other than trans, namely, '∗' is cis (or $0 \pm 55°$), '+' is $90 \pm 35°$ and '-' is $-90 \pm 35°$. A 'B' rotamer tag implies either B0 or B1; and an 'A' tag implies either AR or AT.

Table 5. Structures and thermodynamics of i/i-Met-Enk computed with solvation[a]

index[b]	ncon[c]	$\Delta\overline{F}$[d]	ΔA[e]	S[f]	MC rotamer tags[g]					Motif[h]
1	16731	0.0	0.0	5.5	X	B′	C	A	B	G-P Type II′
2	115	0.2	0.4	5.1	B	AL	AL	B	X	G-G Type I′
3	499	1.4	1.1	6.7	A	A	A	A	B	double bend
4	6450	1.6	1.4	6.6	B	C	A	A	B	G-G Type II′
5	4460	2.2	1.5	8.0	B	C	A	B	X	G-G Type II′
6	4132	3.7	2.2	10.5	B	AL	C	B	X	G-G Type I′
7	8933	4.2	2.4	11.7	B	AL	C	A	B	G-G Type I′
8	1083	3.0	3.0	5.9	B	C	C	A	B	G-G Type I′
9	195	3.0	3.3	4.7	B	C	B	B	X	G-G Type II′
10	37000	0.4	–0.4	8.3	X	X	X	X	X	all conformations

[a] Conformations saved in the MD production step are analyzed. Each row characterizes a group of main chain conformers that possess the structural motif given in the last column.
[b] Conformer number ordered by increasing free energy.
[c] Number of conformations.
[d] Relative Boltzmann averaged total energy (in kcal/mol). See Equation 3.
[e] and [f] See footnotes (d) and (e) to Table 4.
[g] See footnote (f) to Table 4. Conformations of ω that deviate from trans are not resolved. 'X' means any main chain rotamer tag in Figure 1. B′ indicates regions B and AL in Figure 1.
[h] Structural motif based on main chain rotamer tag nomenclature in Table 3.

Table 6. Structure and thermodynamics of n/n-Met-Enk computed with solvation[a]

index[b]	ncon[c]	$\Delta\overline{F}$[d]	ΔA[e]	S[f]	MC rotamer tags[g]					Motif[h]
1	1011	0.0	0.0	3.5	C	C	B	B	X	G-G Type II′
2	6295	1.3	0.6	6.0	B′	C	B	B	X	G-G Type II′
3	400	1.7	0.9	6.3	X	B	C	A	B	G-P Type II′
4	2866	2.5	1.0	8.6	B′	B	C	B	X	G-G Type II
5	222	0.9	1.2	2.5	X	B	C	A	A	G-P Type II′
6	15018	3.5	1.4	10.8	B′	B	B	B	X	extended
7	545	2.7	2.3	4.8	B′	C	B	A	X	G-G Type II′
8	914	4.9	4.4	5.3	B′	C	C	A	X	G-G Type I′
9	4400	6.9	4.7	11.2	B′	C	C	B	X	G-G Type I′
10	28579	1.9	0.2	9.3	B′	B/C	B/C	B	X	2 + 4 + 6 + 9
11	38400	1.0	–0.4	8.3	X	X	X	X	X	all conformations

Footnotes a–h: see Table 5.

is lowest in free energy, but not as populated as other conformers. The other dominant conformers in order of increasing free energy are G-G Type II′ bend, G-G Type II bend extended and G-G Type I′ bend conformers (conformers 2, 4, 6 and 9, respectively). The relative free energy of the extended conformer, which is the most populated (by at least a factor of 2.5), is 1.4 kcal/mol. The extended conformer and the G-G Type I′ bend conformer have the largest entropies. The structures of conformers 2, 4, 6 and 9 differ in the conformation of either Gly 2 or Gly 3, which are either in extended or bend regions of the ϕ/ψ plot in Figure 1. Conformer 10 gives the thermodynamic properties computed for conformations of conformers 2, 4, 6 and 9.

In the R-dielectric calculation of i/i-Met-Enk, a double bend conformer (conformer 1 in Table 7) is lowest in free energy. The other dominant conformers are G-G Type I′, G-P Type II′, G-G Type II′ and G-G Type II bends (conformers 2, 3, 4, and 6, respectively). In the R-dielectric calculation of n/n-Met-Enk, a G-P Type II′ bend conformer (conformers 1 and 2 in Table 8) is lowest in free energy. The other dominant conformers are a G-G Type II bend conformer (conformer 3), an extended conformer (conformer 4), and a G-G Type II′ bend conformer (conformers 5 and 6).

Inter-conversion between conformers of n/n-Met-Enk computed with solvation

For each residue of n/n-Met-Enk, φ/ψ scatter plots of conformations of the extended conformer and three bent conformers (conformers 2, 4, 6 and 9 in Table 6) are plotted in Figure 2. Solid lines are the rotamer region boundaries. According to Figures 2a and 2d, backbone conformations of Tyr 1 and Phe 4 are extended. The two conformations of Met 5 in Figure 2e would be related by symmetry if the C-terminus carboxylic proton were removed. In scatter plots for which the four conformers are plotted separately, conformations of Met 5 populate extended and right-handed α-helix regions about equally; Tyr 1 ψ is in the extended conformation; and a broad range of ϕ values of Tyr 1 are observed, which implies nearly free rotation about the N-terminus C-NH_2 bond. Inter-conversion between conformers is illustrated in the plots for Gly 2 and Gly 3. In Figures 2b and 2c, conformations of Gly 2 and Gly 3 populate region B, which is the region at the top left of the plot, region C, which is the region at the bottom right, and a narrow region that links B and C. In the extended conformation (conformer 6), Gly 2 and Gly 3 both populate region B. In bent conformer 2 of Table 6, Gly 2 populates region C. In bent conformer 4 of Table 6, Gly 3 populates region C. In bent conformer 9 of Table 6, both Gly 2 and Gly 3 populate region C. Inter-conversion between the extended conformer and conformer 2 is due to a change in the conformation of Gly 2 from region B to region C. In the inter-conversion, the value of ϕ changes from -120° to -180° to $-240^\circ = 120^\circ$, and the value of ψ simultaneously changes from 120° to 180° to $240^\circ = -120^\circ$. The conformation of Gly 3 changes in a similar fashion in the inter-conversion between the extended conformer and conformer 4 in Table 6.

The ϕ/ψ-scatter plots of i/i-Met-Enk computed with solvation (plots not given here) support inter-conversion mechanisms between the G-G Type II′

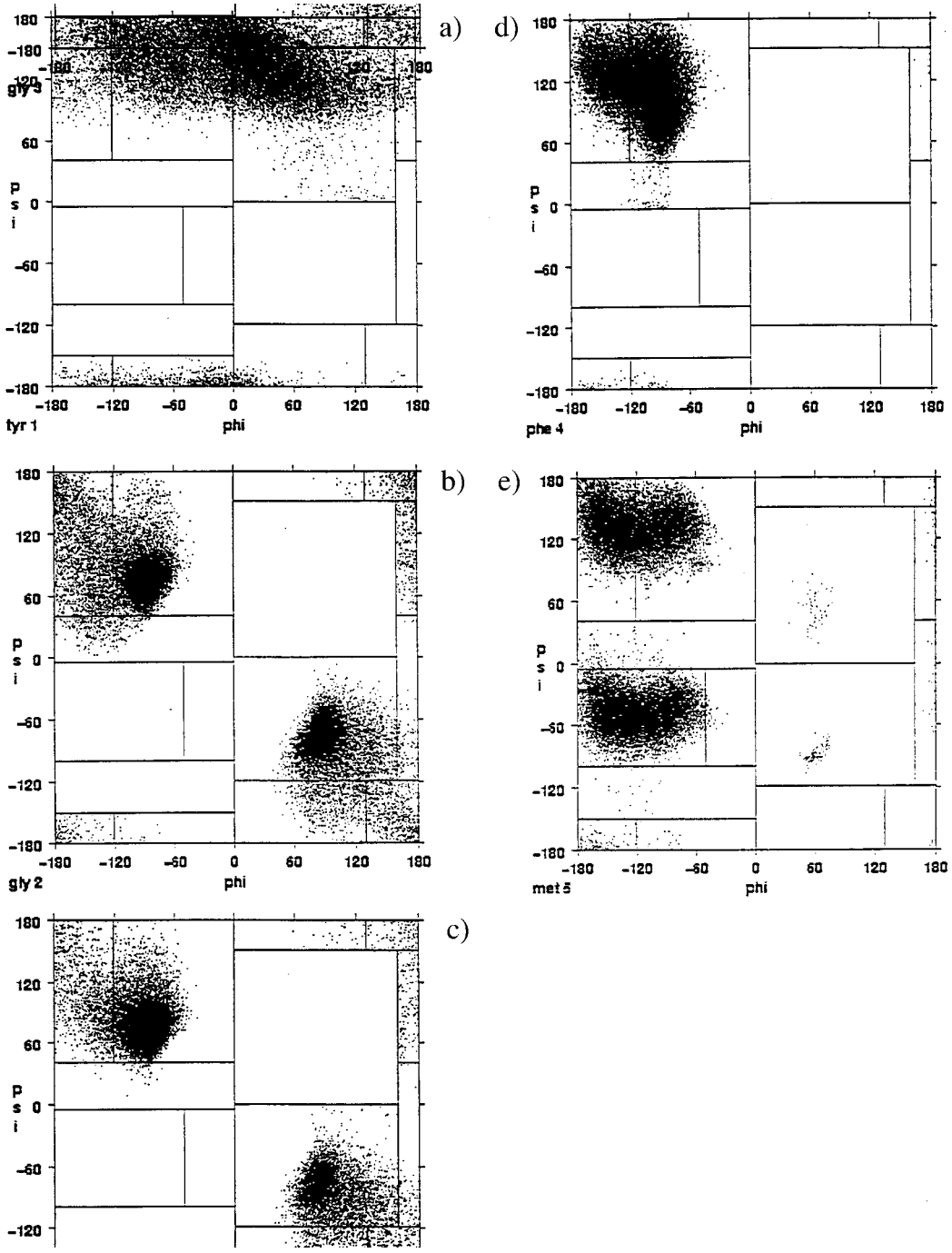

Figure 2. Scatter plots of ϕ/ψ conformations of Tyr 1 (a), Gly 2 (b), Gly 3 (c), Phe 4 (d), and Met 5 (e) of structural motif 6 of n/n-Met-Enk computed with solvation (Table 6). Rotamer region boundaries are illustrated.

Table 7. Structures and thermodynamics of i/i-Met-Enk computed with an R-dielectric[a]

index[b]	ncon[c]	$\Delta\overline{F}$[d]	ΔA[e]	S[f]	MC rotamer tags[g]					Motif[h]
1	1060	0.0	0.0	7.5	A	A	A/C	A	B	double bend
2	6666	1.5	1.4	7.7	B	AL	C	B	X	G-G Type I′
3	9950	2.9	2.9	7.7	X	B	C	A	B	G-P Type II′
4	7330	5.4	4.9	9.4	B	C	A	B	X	G-G Type II′
5	767	5.5	5.6	7.3	B	C	B	B	X	G-G Type II′
6	1267	6.9	7.0	7.2	B	B	C	B	X	G-G Type II
7	139	6.9	8.6	1.9	B	C	C	B	X	G-G Type I′
8	51	9.6	11.3	2.0	B	B	B	B	B	extended
9	38200	0.1	–0.1	8.2	X	X	X	X	X	all conformations

Footnotes a–h: see Table 5.

Table 8. Structures and dynamics of n/n-Met-Enk computed with an R-dielectric[a]

index[b]	ncon[c]	$\Delta\overline{F}$[d]	ΔA[e]	S[f]	MC rotamer tags[g]					Motif[h]
1	1468	0.0	0.0	5.5	X	B	C	A	A	G-P Type II′
2	3777	1.3	0.9	6.7	X	B	C	A	B	G-P Type II′
3	8733	4.0	3.7	6.6	B′	B	C	B	X	G-G Type II
4	2030	4.2	4.6	4.1	B′	B	B	B	X	extended
5	1189	6.6	6.2	7.2	B′	C	B	B	X	G-G Type II′
6	2158	6.7	6.8	5.5	B′	C	A	B	X	G-G Type II′
7	504	10.3	9.8	7.6	B′	C	C	B	X	G-G Type I′
8	34,000	0.2	–0.1	6.8	X	X	X	X	X	all conformations

Footnotes a–h: see Table 5.

bend and G-G Type I′ bend conformers (conformers 5 and 6 in Table 5), which differ in the conformation of the Gly 2 ψ and Gly 3 ϕ dihedral angles, and between the G-G Type II′ bend and G-P Type I′ bend conformers (conformers 1 and 6 in Table 5), which differ in the conformation of the Gly 2 ϕ and Phe 4 ψ dihedral angles.

The ϕ/ψ-scatter plots of i/i-Met-Enk computed with an R-dielectric (plots not given here) support inter-conversion mechanisms between the three dominant conformers in Table 7, the G-G Type I′ bend, G-P Type II′ bend and G-G Type II′ bend conformers (conformers 2, 3 and 4 in Table 7), which involves a mechanism similar to the one in the previous paragraph.

The ϕ/ψ-scatter plots of n/n-Met-Enk computed with an R-dielectric (plots not given here) support a mechanism of inter-conversion between the G-G Type II bend and G-P Type II′ bend conformers (conformers 2 and 3 in Table 8), which differ in the conformation of the Phe 4 ψ dihedral angle, and between two G-G Type II′ bend conformers (conformers 5 and 6 in Table 8), which differ in the conformation of the Gly 3 ψ dihedral angle.

Average conformations of i/i- and n/n-Met-Enk computed with solvation

For solvation calculations of i/i-Met-Enk and n/n-Met-Enk, the lowest energy main chain/side chain conformers associated with dominant motif conformers are characterized in Tables 9 and 10, respectively. Columns 1 to 5 are the conformer number, conformer population, relative total energy, relative free energy and entropy, respectively. Main chain rotamer tags are listed in columns 6 to 10. H-bond patterns observed in the average conformations are reported on the right-hand side of the table. See footnote h to Table 9 for the H-bond criteria.

In the calculation of i/i-Met-Enk, structural motifs of conformers 10, 19 and 82 are G-G Type II′, G-P Type II′ and G-G Type I′ β-turns. The conformation of the lowest energy conformer, a G-P Type II′ bend, lacks Gly 2 to Met 5 H-bonds. Structural motifs of n/n-Met-Enk are the extended chain (conformer 73) and

Table 9. Characterization of main chain/side chain conformers of i/i-Met-Enk computed with solvation[a]

Mer [b]	ncon[c]	$\Delta\overline{F}$[d]	ΔA[e]	S [f]	MC rotamer tags[g]					H-bond pattern[h]
1	11	0.0	0.0	1.4	B1+	B1	C	AR	B0	Y1h1:M5, Y1h2:M5oxt, F4:G2, Y1hh:G3
10	108	2.2	1.9	2.3	B1	C	AR	B0-	B1	[Y1h3:F4, F4:Y1] Y1h1:M5, G2:M5oxt, G3:Y1
19	69	2.5	2.3	2.0	AR	B0	C	AR	B0	[G2:M5, M5:G2] Y1h3:M5oxt
82	81	3.7	3.4	2.6	B1	AL	C	B1	B1	[Y1h1:F4] F4:G2 Y1h2:M5oxt

[a] Lowest energy main chain/side chain conformers of motifs in Table 5 are characterized.
[b] Main chain/side chain conformer number in order of increasing free energy.
[c–f] See footnotes (c) to (f) in Table 5.
[g] See footnote (f) to Table 4. Side chain rotamer tags are not given.
[h] H-bond pattern in average conformation of conformer. Proton donor and acceptor are separated by a colon. Unless indicated otherwise, proton donor is peptide NH and acceptor is peptide carbonyl oxygen. H-bonds in brackets are those expected between anti-parallel strands connected by a β-turn. Residue labels used are one-letter symbol and residue number. Atoms appended to residue labels are: (1) N-terminus hydrogen atoms (h1, h2, h3), (2) Tyr 1 hydroxyl hydrogen (hh) and oxygen (oh), and (3) Met 5 C-terminus hydroxylic hydrogen 'h' and oxygen 'oxt'. H-bond criteria are: (1) H-bond distance less than 2.5 Å, and (2) H-bond angle, $\angle$ (N – H – O), between 120 and 180 °.

Table 10. Characterization of main chain/side chain conformers n/n-Met-Enk computed with solvation[a]

Mer [b]	ncon[c]	$\Delta\overline{F}$[d]	ΔA[e]	S[f]	MC rotamer tags[g]					H-bond pattern[h]
1	3	0.0	0.0	0.5	C	C	B1	B1+	B0	G3:Y1, F4:G2, M5h:Y1oh
2	14	0.6	0.7	0.1	B1	C	B1	B1	B1	G3:Y1, F4:G2, M5:G3
10	13	2.4	1.9	2.1	B1	B1	C	B1	B1	G3:Y1, F4:G2, M5:G3
73	85	4.1	3.2	3.3	AL	B1	B1	B1	B1	G3:Y1, F4:G2, M5:G3
955	6	6.0	6.1	0.2	D	C	C	B0	B0	G3:Y1, F4:G2

[a] Lowest energy main chain/side chain conformers of dominant structural motifs in Table 6 are characterized.
[b-h] See footnotes (b) to (h) in Table 9.

Gly 2 – Gly 3 bend motifs (conformers 1, 2, 10 and 955). H-bond patterns are nearly conserved in the five average conformations.

Boltzmann averaged dihedral angles of conformers characterized in Tables 9 and 10 are given in Table 11. The first column defines the dihedral angles; and the remaining columns give the Boltzmann averaged values. Average conformations of i/i-Met-Enk and n/n-Met-Enk are given under the corresponding entry listed in the first row. Conformation numbers, which are given in the second row, correspond to the conformer numbers in Tables 9 and 10. Relative free energies are reported in the last row. Stereoscopic stick drawings of the average conformations of i/i-Met-Enk and n/n-Met-Enk are depicted in Figures 3 and 4, respectively.

Superimposed stereoscopic stick drawings of average conformations of n/n-Met-Enk are illustrated in Figure 5. Backbone heavy atoms (N, C^{α}, C^{β}, C′ and O) of Phe 4 and Met 5 of conformations 1, 2, 10 and 955 are superimposed on the corresponding atoms of conformation 73. Conformer numbers are placed near the side chains of Tyr 1. For each residue, average rms deviations between backbone, side chain, and all heavy atoms of conformations superimposed are reported in Table 12. The average rms backbone deviation of Phe 4 and Met 5 of conformations 2, 10 and 955 is 0.2 Å. Rms backbone deviations for Gly 3 of conformations 2 and 10 are 0.2 and 0.9 Å, respectively. Conformations 2, 10, and 73 have the same conformation of the Phe 4 side chain (see also χ_1 and χ_2 in Table 11). Conformations 2, 10, 73 and 955 have the same conformation of the Tyr 1 side chain (see χ_1 and χ_2 in Table 11). For conformation 1, the average rms backbone deviation of Phe 4 and Met 5 is 1.3 Å.

Pharmacophore mapping

The average conformation of conformer 1 of n/n-Met-Enk computed with solvation superimposes on the important pharmacophoric groups of morphine [3, 4] (see Gigure 6A) better than the other conformations. The requirements used are geometric constraints implied by the generalized requirements summarized in references 3 and 4. The pharmacophoric requirements

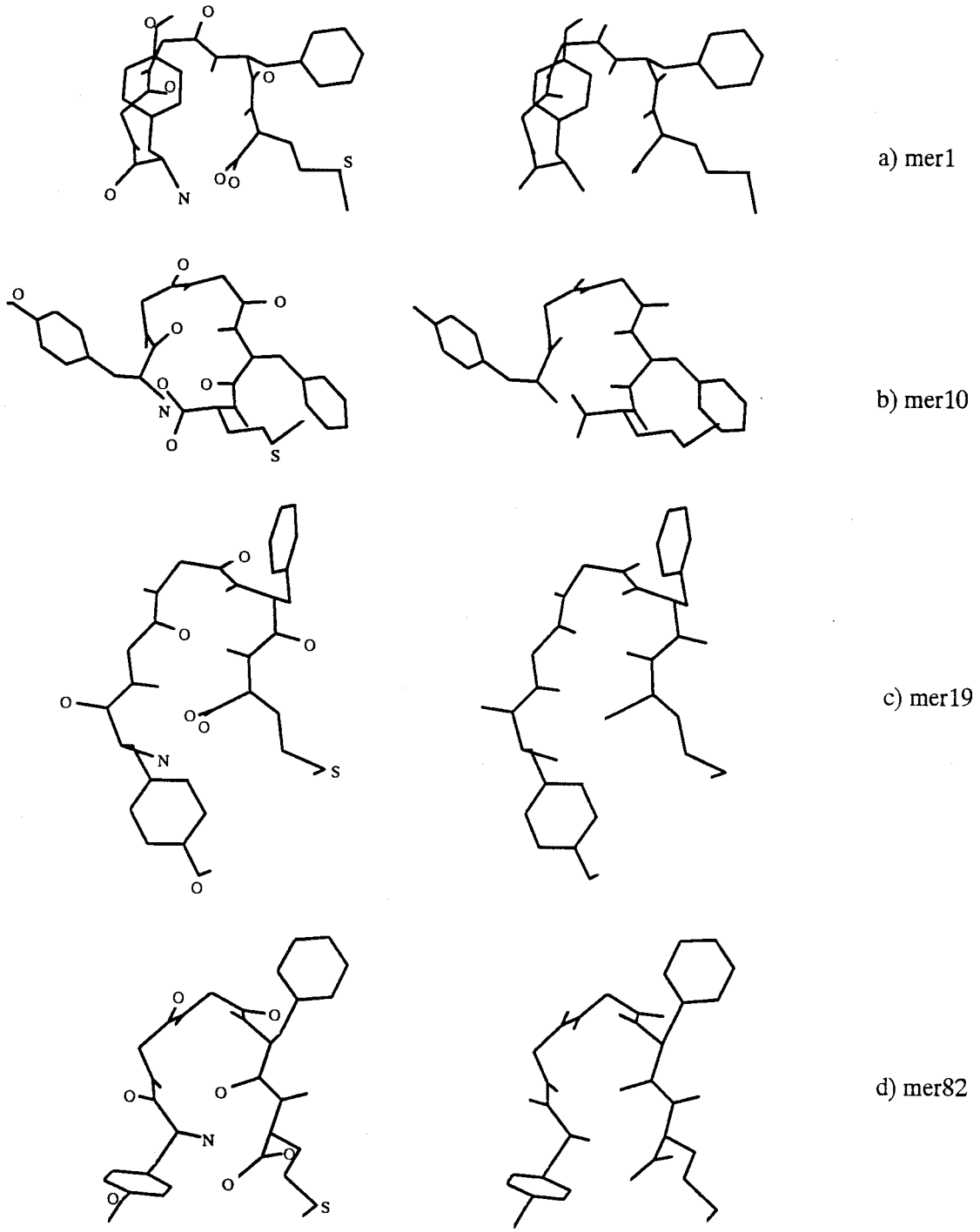

Figure 3. Stereoscopic stick drawings of average conformations of conformers 1 (a), 10 (b), 19 (c) and 82 (d) of i/i-Met-Enk computed with solvation (Tables 9 and 11). Heavy atoms, peptide hydrogen and Tyr 1 OH are depicted. Nitrogen, oxygen and sulfur atoms are labeled.

Table 11. Boltzmann averaged dihedral angles of average conformations[a]

[b]	i/i-Met-Enk[c]				n/n-Met-Enk[c]				
	1	10	19	82	1	2	10	73	955
Tyr ϕ	**–85**	**–101**	**–103**	**–65**	**155**	**–77**	**–52**	**25**	**31**
ψ	**129**	**130**	**–53**	**134**	**–63**	**147**	**169**	**125**	**152**
ω	75	146	167	–163	–149	165	–180	–173	–167
χ_1	–138	–176	–53	–149	–91	–172	–162	–179	–170
χ_2	63	66	105	71	100	81	66	80	87
χ_3	–45	–35	65	108	–86	75	152	16	159
Gly ϕ	**–112**	**89**	**167**	**102**	**66**	**87**	**–84**	**–80**	**72**
ψ	**135**	**–72**	**164**	**76**	**–68**	**–61**	**76**	**73**	**–82**
ω	154	168	170	–177	–180	171	172	174	–177
Gly ϕ	**103**	**–89**	**79**	**81**	**–84**	**–72**	**76**	**–77**	**79**
ψ	**–68**	**–35**	**–90**	**–65**	**73**	**66**	**–84**	**68**	**–74**
ω	–179	178	173	167	–177	–176	–163	175	–163
Phe ϕ	**–89**	**–160**	**–79**	**–91**	**–62**	**–82**	**–91**	**–82**	**–141**
ψ	**–69**	**138**	**–36**	**134**	**126**	**73**	**81**	**87**	**133**
ω	–174	–76	–171	–165	75	177	168	180	–172
χ_1	–170	–170	–55	–69	–89	–75	–77	–66	–175
χ_2	67	79	132	95	90	108	115	112	72
Met ϕ	**–142**	**–73**	**–166**	**–71**	**–163**	**–72**	**–87**	**–99**	**–151**
ψ	**131**	**128**	**110**	**143**	**156**	**136**	**134**	**135**	**133**
ω	–180	–180	–180	–180	–141	168	–178	–178	169
χ_1	178	–64	–173	–155	–131	–62	–168	–69	–88
χ_2	154	–150	163	–155	178	–53	172	170	178
χ_3	132	156	65	–150	140	126	–144	–159	–127
χ_4	44	103	42	65	59	60	49	46	54
ΔA[d]	0.0	1.9	2.3	3.4	0.0	0.7	1.9	3.2	6.1

[a] Boltzmann average conformations of main chain/side chain conformers characterized in Tables 9 and 10 are given.
[b] Dihedral angles of each residue.
[c] Boltzmann averaged dihedral angles of main chain/side chain conformers. Conformations of n/n and i/i-Met-Enk are given. Numbers given across the second row are conformer numbers in Tables 9 and 10.
[d] See footnote (e) to Table 5.

employed here are as follows: (1) The phenyl ring, which is the analogue of the ethylene moiety in ring C of morphine, and Tyr 1 N, which is the analogue of atom N of morphine, are on opposite sides of the plane that coincides with the plane of the phenol ring, which is the analogue of Ring A of morphine; (2) The Tyr 1 N to Tyr 1 OH distance should be close to the N to O1 distance in the morphine crystal structure, 7.1 Å [33]; (3) The Tyr 1 OH to Met 5 O distance should be close to the O1 to O2 distance, 4.6 Å; and (4) The Tyr 1 N to Met 5 O distance should be close to the N to O2 distance, 6.5 Å. Stereoscopic stick diagrams of morphine and a superposition of morphine and the average n/n-Met-Enk conformation based on conformer 1 in Table 11 are illustrated in Figure 6. In the superposition, heavy atoms of Tyr 1, except for C′ and O, are superimposed on corresponding atoms in rings A, B and D; and the Met 5 C′-O bond is superimposed on the C-O2 bond. The average rms deviation of the 12 atoms superimposed is 1.4 Å. In the average conformation, the phenyl ring and Tyr 1 N are on opposite sides of the plane that coincides with the plane of the phenol ring. The Tyr 1 N to Tyr 1 OH distance is 6.8 Å, which deviates from the N to O1 distance in morphine by 0.3 Å. The Tyr 1 OH to Met 5 O and the Tyr 1 N to Met 5 O distances, 3.5 Å and 8.5 Å, respectively, deviate from the corresponding distances in morphine by 1.1 and 2.0 Å, respectively. The three pharmacophoric distances mapped on the peptide are the lengths of the legs of the dashed triangle in Figure 6b.

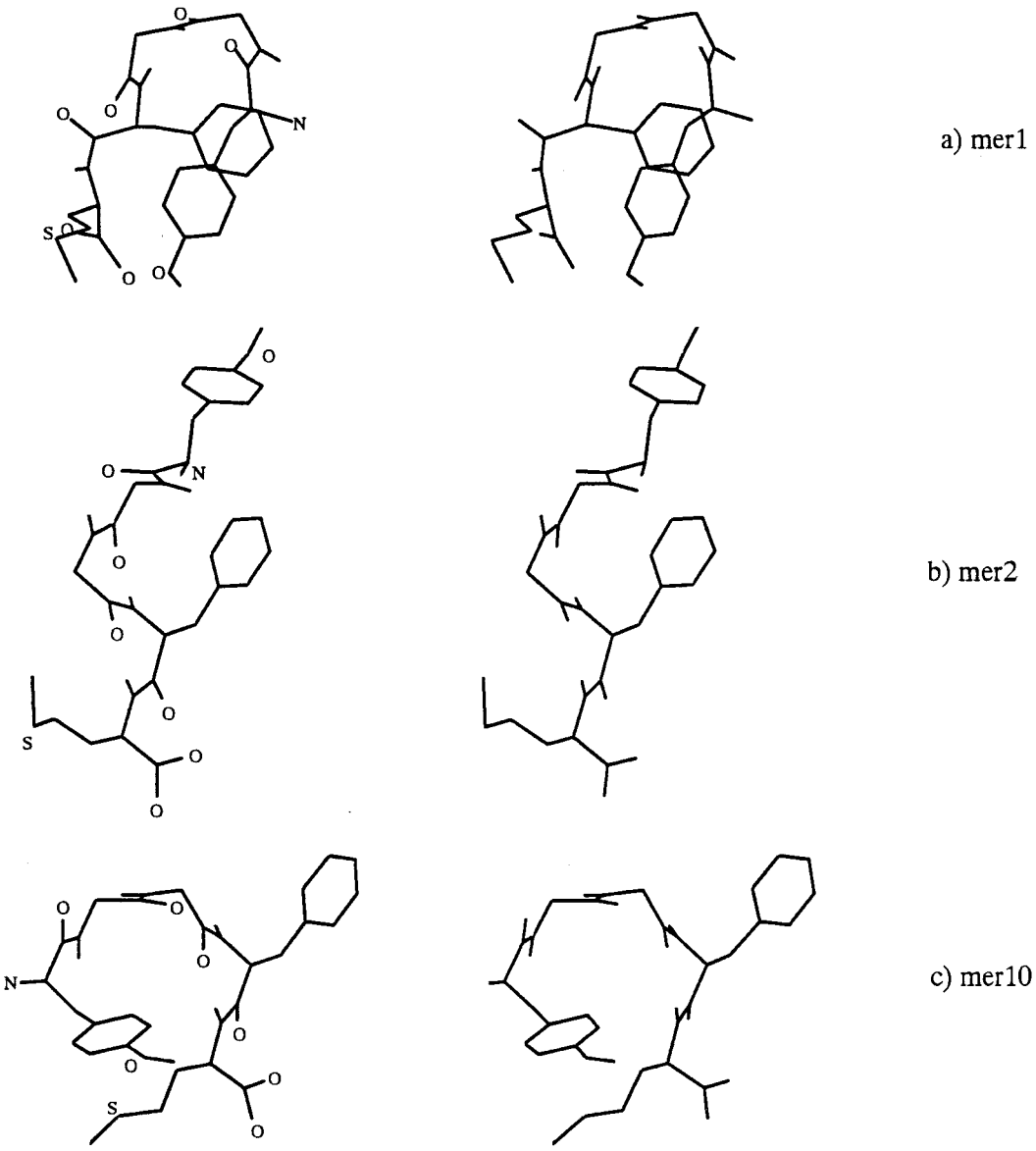

Figure 4. Stereoscopic stick drawings of average conformations of conformers 1 (a), 2 (b), 10 (c), 73 (d) and 955 (e) of n/n-Met-Enk computed with solvation (Tables 10 and 11). See also the caption to Figure 3.

Discussion

The computed structural and thermodynamic properties of the peptide significantly change as the ionization state and the solvent environment are altered. The R-dielectric calculation of n/n-Met-Enk (Table 8) and the solvation calculation of i/i-Met-Enk (Table 5) are the calculations that should be used to describe the peptide in lipid and aqueous environments, respectively. Dominant motif conformers common to both 'aqueous solution' and 'lipid' calculations are the G-P Type II′ bend conformer, which is the lowest free energy conformer in both calculations (conformer 1 in Tables 5 and 8), and the G-G Type II′ bend conformer (conformers 4 and 5 in Table 5, and conformer 6 in Table 8). The G-P Type II′ bend conformer corresponds to the global minimum energy conformation computed previously [11]. The G-G Type I′ bend conformer is a dominant conformer found only in the 'aqueous solution' calculation. The dominant conformers computed

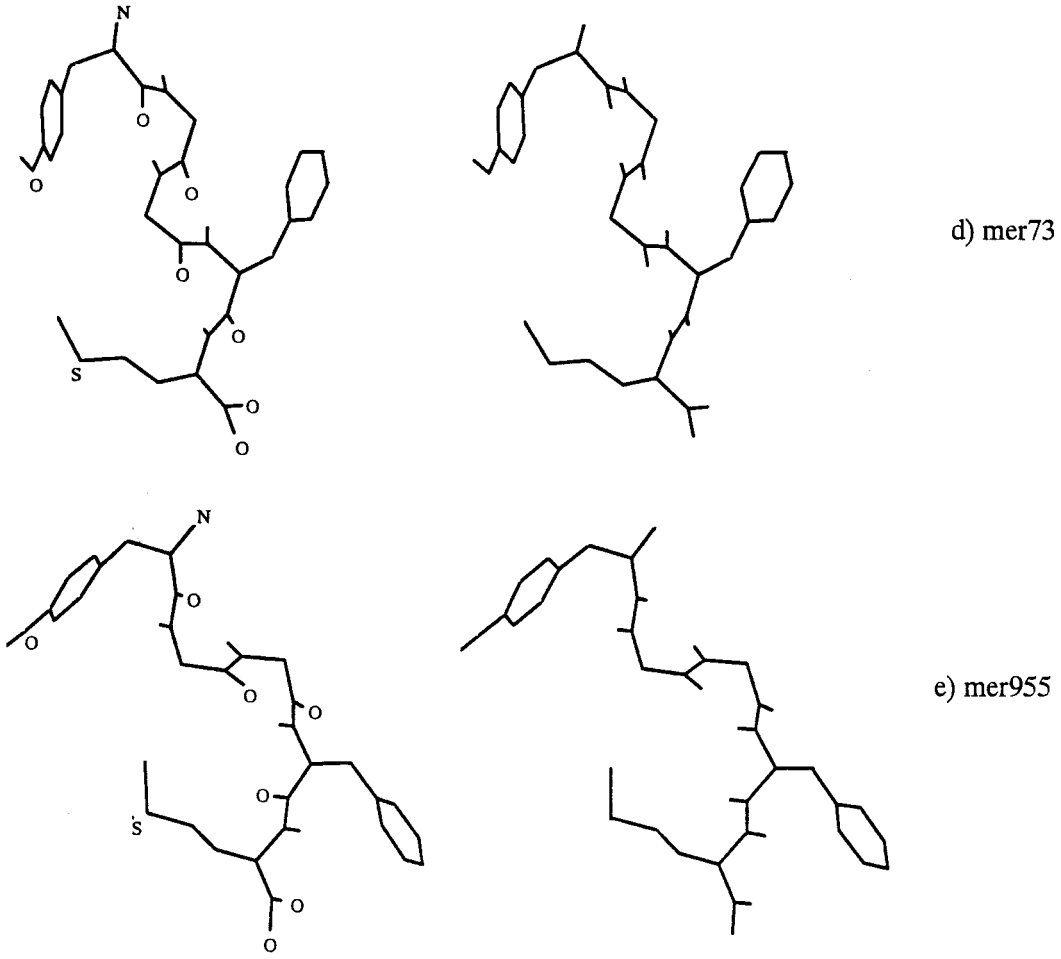

Figure 4. (Continued).

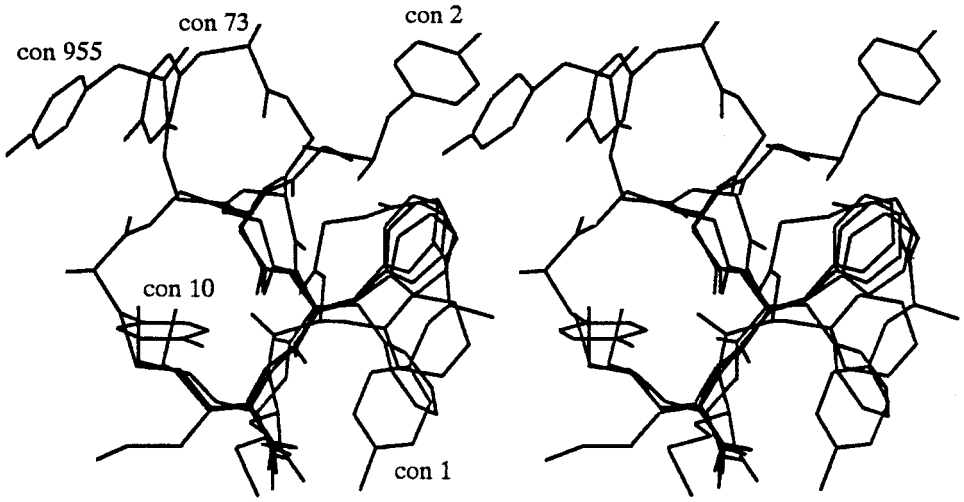

Figure 5. Superimposed stereoscopic stick drawings of average conformations of conformer 1, 2, 10, 73 and 955 of n/n-Met-Enk (Tables 10 and 11). Only heavy atoms are depicted. Conformer labels appear next to the phenol ring.

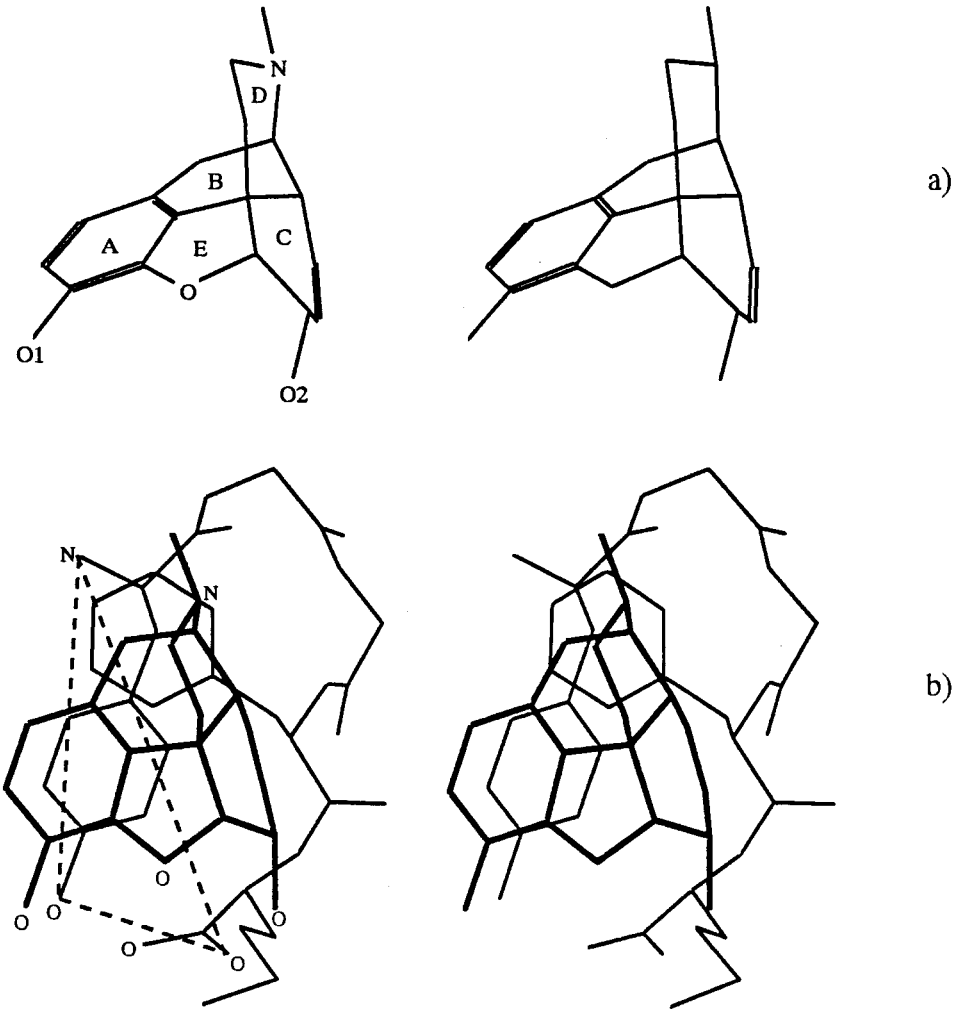

Figure 6. Stereoscopic stick drawings of morphine (a) and average conformation of conformer 1 of n/n-Met-Enk (Tables 10 and 11) superimposed on morphine (b). Nitrogen and oxygen atoms, and rings in morphine are labeled. In the average conformation, Tyr 1 N, oxygen of phenol, and C-terminus oxygen atoms are labeled.

Table 12. Rms deviations between superimposed average conformations of n/n-Met-Enk[a]

res[b]	Conformer 1			Conformer 2			Conformer 10			Conformer 955		
res[b]	ALL[c]	BACK[d]	SIDE[e]	ALL[c]	BACK[d]	SIDE[e]	ALL[c]	BACK[d]	SIDE[e]	ALL[c]	BACK[d]	SIDE[e]
Tyr 1	11.8	9.9	12.9	8.3	5.2	9.9	8.0	8.2	7.9	4.0	3.9	4.0
Gly 2	4.9	4.9	0.0	1.5	1.5	0.0	4.2	4.2	0.0	3.8	3.8	0.0
Gly 3	2.5	2.5	0.0	0.2	0.2	0.0	0.9	0.9	0.0	1.6	1.6	0.0
Phe 4	3.2	1.3	4.1	0.3	0.2	0.4	0.6	0.1	0.8	3.8	0.4	5.2
Met 5	4.2	1.3	6.1	1.3	0.2	1.9	2.0	0.1	3.0	0.7	0.4	1.0

[a] Rms deviations between heavy atoms of average conformations of main chain/side chain conformers and average conformation of conformer 73 in Table 10. Conformer numbers are given across the first row. Backbone heavy atoms of Phe 4 and Met 5 are superimposed.
[b] Residue and sequence number.
[c] Rms deviation between all heavy atoms.
[d] Rms deviation between backbone atoms N, C^{α}, C^{β}, C′ and O.
[e] Rms deviation between side chain heavy atoms beyond C^{β}.

only in the 'lipid' calculation are the G-G Type II bend conformer and the extended conformer.

In a comparison of the use of solvation free energy versus just an R-dielectric, the dominant motif conformers of i/i-Met^5-Enk (Tables 5 and 7) are the same; and most of the dominant motif conformers of n/n-Met-Enk (Tables 6 and 8) are the same. The relative free energy order of the dominant conformers changes as the solvent environment is altered. Compared to R-dielectric calculations, dominant conformers computed with solvation have larger populations; the entropy contribution to conformer stability, which increases with the density of conformational states, is greater in solvation calculations; and the relative free energies are closer together, which implies a larger density of conformer states in solvation calculations. The entropies of dominant conformers differ by as much as 8 cal K^{-1} mol^{-1} in solvation calculations, and 3 cal K^{-1} mol^{-1} in R-dielectric calculations.

The calculations support the proposition that the net charges at the N- and C-termini are neutral (or reduced) in the receptor (or crystal) environment. The proposition is supported by the following computational results: (a) the extended conformer becomes a dominant conformer in the apolar calculation of n/n-Met-Enk, (b) the use of solvation in the calculation of n/n-Met-Enk significantly increases the population of the extended conformer (by at least a factor of 2.5) relative to the bent conformers, and (c) the average conformation of a low free energy bent conformer of n/n-Met-Enk computed with solvation superimposes well on the important pharmacophoric groups in morphine. Solvation calculations of the peptide with neutral N-terminus and ionized C-terminus, and with ionized N-terminus and neutral C-terminus (data not reported here), show that the neutral state of the peptide N-terminus induces and stabilizes the extended conformation. Calculations that employ various dielectric constants and reduced net charges on the N- and C-termini have been performed. In R-dielectric calculations, a 40% reduction in net charge at the N-8 C-termini induces the extended conformation of i/i-Met-Enk.

In calculations of n/n-Met-Enk, the fraction population of the extended conformer is 39% when computed with solvation compared to only 6% when computed with just an R-dielectric. In solvation and R-dielectric calculations of i/i-Met-Enk, no dominant extended conformers are observed. Two factors that affect the population of a conformer are interconversion with lower energy conformers, and the accessibility of the extended conformer to high energy conformational states, which increases with the opening at the top of the potential energy well. The former mechanism is probably not so significant seeing that the MD runs do not produce a Boltzmann distribution of conformer populations. The larger population of the extended conformer in the solvation calculation is likely due to increased accessibility of the extended conformer brought on by stabilization of exposed backbone polar atoms. The use of solvation free energy versus just an R-dielectric reduces the relative free energy of the extended conformer from 4.6 kcal/mol to 1.4 kcal/mol. In the crystal structure, H-bonds between peptide molecules of the pleated sheet [34] should lower the free energy of the extended conformer relative to bent conformers even more.

In the solvation calculation of n/n-Met-Enk, the average conformation of a low free energy conformer, a G-G Type II′ bend (conformer 1 in Tables 10 and 11 and Figures 4 and 6), superimposes well on the important pharmacophoric groups in morphine. The phenyl ring and Tyr 1 N are on opposite sides of the plane that coincides with the plane of the phenol ring. The Tyr 1 OH to Tyr 1 N distance deviates from the corresponding distance in morphine by only 0.3 Å. A conformation similar to that of conformer 1 in Tables 10 and 11 has not been previously reported to the best of the author's knowledge.

The conformational analysis of n/n-Met-Enk computed with solvation supports a mechanism of interconversion between the extended conformer and three bent conformers. In ϕ/ψ-scatter plots of conformations of conformers 2, 4, 6 and 9 (Figure 2), Gly 2 and Gly 3 conformations are uniformly distributed in a narrow region that connects the extended region (regions B0 and B1 in Figure 1) with a turn region (region C). In the ϕ/ψ scatter plots of the extended conformer and any other bent conformer (conformer 2, 4, or 9), the distributions of conformations appear just as uniform as they do in Figure 2 (plots not given here). The free energies of three conformers, G-G Type II′ bend, G-G Type II bend, and extended conformers (conformers 2, 4, and 6 in Table 6), are within 0.8 kcal/mol. The entropy contribution to the free energy of stabilization of the extended conformer relative to the next most populated conformer (conformer 2 in Table 6) is –1.4 kcal/mol at 25 °C; and the average total energy of the extended conformer is 2.2 kcal/mol higher. The main chain conformation of the extended conformer differs from that of the G-G Type II′ bend conformer and the G-G Type II bend conformer in the

conformations of just Gly 2 and Gly 3, respectively. The lowest free energy conformer, which superimposes well on the important pharmacophoric groups in morphine, does not easily inter-convert with the dominant conformers (based on ϕ/ψ-scatter plots not given here). Based on ϕ/ψ-scatter plots of Met-Enk computed with solvation and computed with just an R-dielectric, inter-conversion between dominant conformers appears easier when solvation free energy is employed in the calculation.

The populations of dominant conformers in Tables 5 to 8 do not have a Boltzmann distribution. Due to the use of multiple independent MCSA conformational searches to generate starting conformations for MD runs, all the conformers generated do not inter-convert. Failure of conformer inter-conversion would prevent equilibration during the MD runs. The relative free energies of the dominant conformers are not very large, especially in the solvation calculations. The conformer relative free energies and populations could change with improvements in the approximations employed, namely, the use of fixed bond lengths and bond angles, the use of Lennard-Jones, electrostatic and torsion potentials in Equation (1), the use of solvation free energy based on solvent accessible surface area, and the absence of explicit water, salt and ionic species. A thorough examination of the approximations employed is beyond the scope of this study. The computed thermodynamic properties of dominant conformers that easily inter-convert should be most useful.

The calculation by Ishida et al. [18] and the R-dielectric calculation of i/i-Met-Enk (Table 7) are similar. Ishida analyzed conformations collected during MD simulations using the program AMBER [35] and starting from the extended conformation. The lowest energy conformation computed, a G-G Type II′ β-turn, corresponds to conformer 4 in Table 7, for which the relative free energy is 4.9 kcal/mol. In this study, dominant motif conformers lower in free energy are a double bend, a G-G Type I′ bend, and a G-P Type II′ bend (conformers 1, 2 and 3 in Table 7). In the G-G Type II′ β-turn structure described by Ishida et al. as satisfying their pharmacophoric requirements for bioactivity, the phenyl ring and Tyr 1 N pharmacophores are on the same side of the plane that coincides with the plane of the phenol ring, which does not agree with the pharmacophoric requirements employed here.

The R-dielectric calculation in the study by Perez et al. [19] and the R-dielectric calculation of n/n-Met-Enk (Table 8) are similar. Perez et al. employed high temperature conformational searches using the CHARMm parameter set. In the Perez calculation, all geometric parameters can vary; and energy minimization is employed in the final optimization step. In the present study, bond lengths and bond angles are held fixed; and average conformations are generated from MD runs. Conformers 1, 2, 3, and 8 in the Perez study are G-P Type II′ β-turn conformers. Conformers 1, 2 and 3 of Perez correspond to conformer 2 here; and conformer 8 of Perez corresponds to conformer 1 here. The present calculation produces two dominant conformers not found by Perez, namely, the G-G Type II and G-G Type II′ bend conformers (conformers 3, 5, and 6). Perez et al. set the C-terminus C′-OH bond torsion potential equal to zero. As a result, the lowest energy conformer has a cis conformation of Met 5 ω. In this study, the C^{α}-C′-O-H torsion parameter, $U_0/2$, is 1.2 kcal/mol; and values of Met 5 ω are in the range $180 \pm 90\,^{\circ}$. Conformations obtained in polar ($\epsilon = 80$) calculations by Perez do not correspond with any of the conformers of n/n-Met-Enk computed with solvation in Table 6.

The ensemble conformations can be used to estimate upper limits of unbinding free energy and entropy. The assumptions are as follows: (1) The ensemble entropy does not significantly change as the number of MD runs is increased, (2) The free peptide conformation is described by the ensemble conformations (last row of Table 5), and (3) The enzyme bound state is a rigid conformation, for which the computed entropy is zero. Based on the ensemble entropy of i/i-Met-Enk, the entropy contribution to the free energy of unbinding can be as large as -2.5 kcal/mol at 25 °C. The estimated unbinding entropy neglects the entropy of the relaxation processes that take place at the enzyme receptor once the peptide is released, and the thermodynamics of hydration of polar and nonpolar groups.

The ensemble entropy is similar in magnitude to the experimental entropy of unfolding of globular proteins. Based on calorimetric measurements, the entropy of reversible unfolding in aqueous solution at 25 °C is 1.9 cal K^{-1} (mol residue)$^{-1}$ for barnase [36, 37], and –0.2 cal K^{-1} (mol residue)$^{-1}$ for ubiquitin [38]. Both proteins do not have disulfide bridges. The unfolding entropy includes the entropy due to hydration of polar and nonpolar groups, which is very significant according to Makhatadze and Privalov [21]. In the solvation calculation of i/i-Met-Enk, the ensemble entropy is 8.3 cal K^{-1} mol^{-1}, or 1.7 cal K^{-1}

(mol residue)$^{-1}$ (conformer 10 in Table 5). The computed entropy is the sum of the configuration entropy and the entropy due to the correlation between peptide configuration and hydration.

Conclusions

The thermodynamic properties of the conformational states of Met-Enk are understood in terms of the peptide ionization state and solvent environment. The results of solvation calculation of n/n-Met-Enk agree with experimental observations. In the solvation calculation of n/n-Met-Enk, the extended conformation of the peptide, which is the only solid state structure known, is 2.5 times more populated than the next dominant conformer, and only 1.4 kcal/mol in relative free energy; and a low free-energy conformer superimposes well on the important pharmacophoric groups of morphine. In the solvation calculation of n/n-Met-Enk, ϕ/ψ scatter plots and relative free energies support a mechanism of inter-conversion between the extended conformation and three bent conformations. The conformational search employed discovered dominant conformers not previously computed. The knowledge and experience obtained in the present study should be useful in studies on short peptides and flexible protein surface loops.

Acknowledgements

Discussions with colleagues at USF are gratefully appreciated. Reviewers comments are gratefully appreciated.

References

1. Hughes, J., Smith, T.W., Kosterlitz, H.W., Fothergill, L.A., Morgan, B.A. and Morris, H.R., Nature, 258 (1975) 577.
2. Schwyzer, R., Biopolymers, 37 (1995) 5.
3. Schiller, P.W., In Udenfriend, S. and Meihofer, J. (Eds.) The Peptides, Vol. 6, Academic Press, Orlando, FL, 1984, pp. 219–268.
4. Hansen, P.E. and Morgan, B.A., In Udenfriend, S. and Meihofer, J. (Eds.) The Peptides, Vol. 6, Academic Press, Orlando, FL, 1984, pp. 269–321.
5. Deschamps, J.R., George, C. and Flippen-Anderson, J.L., Biopolymers (Peptide Science), 40 (1996) 121.
6. Garbay-Jaureguiberry, C., Roques, B.P., Oberlin, R., Anteunis, M. and Lala, A.K., Biochem. Biophys. Res. Commun., 71 (1976) 558.
7. Jones, C.R., Gibbons, W.A. and Garsky, V., Nature, 262 (1976) 779.
8. Roques, B.P., Garbay-Jaureguiberry, C., Oberlin, R., Anteunis, M. and Lala, A.K., Nature, 262 (1976) 779.
9. Khaled, M.A., Long, M.M., Thompson, W.D., Bradley, R.J., Brown, G.B. and Urry, D.W., Biochem. Biophys. Res. Commun., 76 (1977) 224.
10. Graham, W.H., Carter, E.S. and Hicks, R.P., Biopolymers, 32 (1992) 1755.
11. Isogai, Y., Nemethy, G. and Scheraga, H.A., Proc. Natl. Acad. Sci. USA, 74 (1977) 414.
12. Li, Z. and Scheraga, H.A., Proc. Natl. Acad. Sci. USA, 84 (1987) 6611.
13. Purisima, O. and Scheraga, H.A., J. Mol. Biol., 84 (1987) 6611.
14. Moskowitz, J.W., Schmidt, K.E., Wilson, S.R. and Cui, W., Int. J. Quant. Chem. Quant. Chem. Symp., 22 (1988) 611.
15. Ripoll, D.R. and Scheraga, H.A., J. Protein Chem., 8 (1989) 263.
16. Kawai, H., Kikuchi, T. and Okamoto, Y., Protein Eng., 3 (1991) 85.
17. Morales, L.B., Garduño-Juárez, R. and Romero, D., J. Biomol. Struct. Dyn., 8 (1991) 721.
18. Ishida, T., Yoneda, S., Doi, M., Inoue, M. and Kitamura, K., Biochem. J., 255 (1988) 621.
19. Perez, J.J., Villar, H.O. and Loew, G.H., J. Comput.-Aided Mol. Design, 6 (1992) 175.
20. Richardson, J., Adv. Protein Chem., 34 (1981) 167.
21. Makhatadze, G.I. and Privalov, P.L., Protein Sci., 5 (1996) 507.
22. Carlacci, L. and Englander, S.W., J. Comput. Chem., 17 (1996) 1002.
23. Carlacci, L. and Englander, S.W., Biopolymers, 33 (1993) 1271.
24. Némethy, G., Pottle, M.S. and Scheraga, H.A., J. Phys. Chem., 87 (1983) 1883.
25. CHARMm is a trademark of Molecular Simulations.
26. Vila, J., Williams, R.L., Vasquez, M. and Scheraga, H.A., Proteins Struct. Funct. Genet., 10 (1991) 199.
27. Wesson, L. and Eisenberg, D., Protein Sci., 1 (1992) 227.
28. Perrot, G., Cheng, B., Gibson, K.D., Vila, J., Palmer, K.A., Nayeem, A., Maigret, B. and Scheraga, H. A., J. Comput. Chem., 13 (1992) 1.
29. Metropolis, N., Rosenbluth, A.W., Rosenbluth, M.N., Teller, A.H. and Teller, E., J. Chem. Phys., 21 (1953) 1087.
30. Ponder, J.W. and Richards, F.M., J. Mol. Biol., 193 (1987) 775.
31. Sibanda, B.L., Blundell, T.L. and Thornton, J.M., J. Mol. Biol., 206 (1989) 759.
32. Wilmot, C.M. and Thornton, J.M., J. Mol. Biol., 203 (1988) 221.
33. Gylbert, L., Acta Crystallogr. Sect. B, 29 (1973) 333.
34. Griffin, J.F., Langs, D.A., Smith, G.D., Blundell, T.L., Tickle, I.J. and Bedarkar, S., Proc. Natl. Acad. Sci. USA, 83 (1986) 3272.
35. Weiner, S.J., Kollman, P.A., Nguyen, D.T. and Case, D.A., J. Comput. Chem., 7 (1986) 230.
36. Griko, Y.V., Makhatadze, G.I., Privalov, P.L. and Hartley, R.W., Protein Sci., 3 (1994) 669.
37. Martinez, J.C., elHarrous, M., Filimonov, V.V., Mateo, P.L. and Fersht, A.R., Biochemistry, 33 (1994) 3919.
38. Wintrode, P.L., Makhatadze, G.I. and Privalov, P.L., Proteins Struct. Funct. Genet., 18 (1994) 246.